Dissipation of traffic jams using a single autonomous vehicle on a ring road

Amaury Hayat, Benedetto Piccoli, Sydney Truong

Dissipation of traffic jams using a single autonomous vehicle on a ring road

Amaury Hayat[a,b], Benedetto Piccoli[a], and Sydney Truong[a]

[a]Department of Mathematical Sciences and Center for Computational and Integrative Biology, Rutgers University–Camden, 303 Cooper St, Camden, NJ, USA
[b]CERMICS, Ecole des Ponts ParisTech, Champs-sur-Marne, France

Abstract

In this article, we study the problem of stabilizing the traffic flow on a ring road to a uniform steady-state using autonomous vehicles (AV). Traffic is represented at microscopic level via a Bando-Follow-the-Leader model capable of reproducing phantom jams. For the single-lane case, a single AV can stabilize an arbitrary large ring road with an arbitrary large number of cars. Moreover, this stabilization is exponentially quick with a decay rate independent of the number of cars and control gain also independent of the number of cars. On the other side, the stabilization domain and stabilization time depend on the number of cars.
Two types of controller algorithms are proposed: a proportional control and a proportional-integral control. In both cases, the measurements used by the controller only depend on the local data around the AV, enabling an easy implementation. After numerical tests of the single-lane case, a multi-lane model is described using safety-incentive mechanism for lane change. Numerical simulations for the multi-lane ring road suggest that the control strategy is also very efficient in such setting, even with a single AV.

1 Introduction

Ring-road systems are usually considered as a good first step to understand traffic flows behavior and design efficient controllers to stabilize traffic flows. The underlying reason is that several experimental observations have shown that this system can spontaneously generate stop and go waves [34, 36, 39, 33]. These stop and go waves are at the origin of traffic congestion and prevent the system from reaching or staying in the ideal case: a uniform-flow steady-state. Doing so, they drastically increase the energy consumption and CO2 emission as the drivers have to brake and accelerate continuously. They also have a negative psychological impact on drivers and are mostly seen as a stressful driving situation [11]. Being able to smoothen and stabilize the system when such stop and go waves occur is very interesting from an application perspective, and many studies have tried to tackle this problem with different controllers. For instance, a classical strategy consists of using ramp metering or junctions as a boundary control on the system [35, 26, 4, 16] or using variable speed limits as a means of control [18]. The rapid technological developments allow to consider Autonomous Vehicles (briefly AVs) or Advanced Driver Assistance Systems (briefly ADAS) as ways of influencing traffic. For our considerations, we assume that an automatic feedback can be implemented by AVs of via ADAS, based on information available on board of the vehicles. In other words, the feedback control act independently and in a distributed fashion, using only local information on a selected number of vehicles. The percentage of these vehicles as part of the overall traffic is called penetration rate, and we aim at using a low penetration rate not exceeding 5%. In all our results, we will use just one AV in a ring road with N human-driven cars, thus the penetration rate will be $1/(N+1)$.
The specific control problem we address is the stabilization of uniform-flow steady-state using an autonomous vehicle as a controller. Using AVs to control traffic flows in the framework of mixed human-AV traffic has emerged in the recent years [37, 38] (see for instance [10] for a more detailed review). Several approaches

have been studied: macroscopic [12, 9, 29], mean-field games [19], microscopic [10, 7], etc. In this paper, we consider a microscopic approach with $N+1$ cars. We assume that N cars are human-driven, while one of the cars is an AV whose acceleration can be prescribed. The behavior of the human-driven cars is modeled by the Bando-Follow The Leader (or Optimal Velocity-Follow The leader) model. This model combines an optimal velocity part derived in [3] which represents the incentive of a driver to reach its "own" optimal velocity depending of the space between his vehicle and the vehicle in front, and a "Follow the Leader" part proposed in [13] which represent the incentive of the driver to mimic the vehicle in front. This model has been shown to accurately reproduce stop and go waves for a ring-road in [7, 10], both theoretically and numerically. Such problem on a ring road was considered in [10] where the authors proved the controllability and stabilization of the system with local controls when the road had up to $N = 9$ cars. They designed a proportional and proportional-integral feedback control that seemed efficient in numerical simulations and suggested that the stabilization could also hold for around 20 vehicles. In [7], the authors proposed another controller, and by carefully analyzing the transfer function, they showed that it asymptotically stabilizes the system for any number of cars for arbitrarily large N. However, they were not in position of designing explicit gains and showed that the control gain of their controller was scaling exponentially quickly with N, for N large. In [40] the authors study a similar problem but with a simpler microscopic model and reaches similar conclusion, showing in addition the controllability of the linearized system. However, they were also not in a position of designing explicit gains. In this article, we propose another control strategy to tackle these limitations.

1.1 Contribution of the paper

Adding a single AV could seem to be a very weak action on the system, especially if the number of human-driven vehicles N is arbitrary and could become very large. In this case, the penetration rate (i.e. the percentage of AVs in bulk traffic) would become as small as desired. However, we show that, as in [33], this very weak action is enough to get the exponential stability of all steady-states when using a proportional or a PI controller. More suprisingly, the maximal exponential decay rate is uniform, irrespective of the total number of cars N, and the control amplitude can also be chosen independently of the number of cars. This last point is of paramount importance when dealing with practical system as the AV presents a physical bound on achievable accelerations (both positive and negative). Also, the condition we give on the proposed proportional and PI controllers are optimal (necessary and sufficient).

We then provide an estimation of the basin of attraction, which decays as the number of vehicle increases, as expected. Finally, the time needed to stabilize the system increases with the number of cars: this seems hard to avoid due to the finite propagation speed of the information in the system. However, we show that it scales linearly with time, which is what would be intuitively hoped for in ideal cases. When a non-constant disturbance occurs and prevent the existence of a steady-state, we show that we can still derive an exponential Input-to-State Stability estimate. Input-to-State stability is a more generic notion than exponential stability which measures the resilience of the stability of a system to external and time varying disturbances (see Section 2 or [32] more details). This notion is important as external disturbances to the model always happen in practical applications. In traffic for instance they could represent defect of the model compared with a real or particular individual driver's behavior, measurements error, etc.

We also test our controller in a multi-lane setting. More precisely, we consider a ring road with three lanes, where the vehicles can change lanes according to some lane-changing rules. There is a large literature on how to model lane changing mechanism and its impact on the traffic [22, 24, 20, 21], and here we use a modification of the model proposed in [22]: a vehicle changes lane when three conditions are satisfied: it is safe to do so (changing lane will not produce a strong braking) ; its acceleration in the new lane will be higher than in its original lane ; it has not changed lane in a reasonable amount of time. We provide numerical simulations showing that, interestingly, we can considerably stabilize the three lanes with a single AV, that is allowed to change lanes with a lateral control law that we give in Section 4. This lateral control is designed to create an incentive for the AV to be in the lane of higher speed variance, while making sure that the AV does not change lane to often. Because of the possibility to lane-change the system is hybrid, which makes its theoretical study largely open [15, 14, 27]. This is an incentive for more theoretical studies

on these controllers in a multilane setting as well as implementations on a multilane road.

This paper is organized as follows: in Section 2 we state the main results, which are proved in Section 3. Finally, in Section 4 we provide numerical simulations.

2 AV stabilizing controllers for a ring road

We consider a ring road of length L with N vehicles and one AV, and we denote by $(x_i, v_i)_{i\in\{1,\dots,N\}}$ the position and velocities of the vehicles and (x_{N+1}, v_{N+1}) the position and velocity of the AV. The vehicles are modeled by the following combined Bando (or Optimal Velocity) - Follow The Leader Model [3, 13]:

$$\begin{aligned} \dot{x}_i &= v_i, \\ \dot{v}_i &= a\frac{v_{i+1}-v_i}{(x_{i+1}-x_i)^2} + b[V(x_{i+1}-x_i)-v_i], \end{aligned} \quad 1 \le i \le N \tag{2.1}$$

where a and b are two positive parameters weighting respectively the strength of the Follow The Leader part and the Bando part of the model, and V is the optimal velocity of the Bando model. A way to choose realistic coefficients a and b were studied in detail in [28]. Usually V is taken as an increasing function of the form of a ratio of hyperbolic tangents. However, we will not make any such assumptions here and only assume that V is a differentiable, nonnegative and increasing function. The increasing assumption is dictated by the physical fact that the more distance there is between the vehicles, the more likely the vehicles try to have a large speed. We aim at stabilizing the system to a steady-state in speed, with all cars moving at same speed $\bar{v}$. From (2.1), the only steady-state is $\bar{v} = V(L/N)$. Without controller, the system is closed by considering that the $N+1$-th vehicle is the first vehicle, due to the ring road structure and therefore taking $v_{N+1} = v_1$ and $x_{N+1} = x_1$ in (2.1). This system can have both stable and unstable regime depending on the parameters a, b, and V, and the car density $d^{-1} = N/L$. In particular, the following was shown in [7].

Proposition 2.1. *If*

$$\frac{b}{2} + (\frac{a}{d^2}) < V'(d) \tag{2.2}$$

then the system (2.1) *is unstable.*

Remark 2.1. In particular this implies that there exists there exists $N_1 > 0$ such that if $N > N_1$ the steady-state of the uncontrolled system (2.1) is unstable.

This theoretical proposition explains the instabilities that are observed both in numerical simulations (see Section 4) and in experimental results [34]. Adding an AV to the system, and controlling its acceleration, the dynamics is given by

$$\begin{aligned} \dot{x}_{N+1} &= v_{N+1} \\ \dot{v}_{N+1}(t) &= u(t), \end{aligned} \tag{2.3}$$

where u is the control. We will use u as a feedback control. Using a feedback control means that the controller has to depend on the current state of the system. For instance it can depend on the current velocity of the AV as we do later on. One could why not using an open-loop control instead, where u would depend only on time and the initial conditions of the system. This would avoid having to know the state of the system at each timestep. However, this might not be robust to small perturbations on the state of the system or on the model. This last point is quite important as traffic models are only imperfect approximation of the real behaviors of drivers. This motivates our choice of using a feedback controller. In addition we are aiming to design a very simple feedback control, depending only on local measurements around the AV, in order to enable a practical and decentralized implementation. Therefore, we look for a proportional feedback of the form

$$u(t) = k(\bar{v} - v_{N+1}), \tag{2.4}$$

where k is a tuning parameter. We later extend this control and consider a proportional-integral (PI) feedback law, see Section 2.1. Finally, in Section 4, we modify this controller to account for larger perturbations. The system with control (2.4) presents several admissible steady states given by

(A1) The steady speed $\bar{v}$ is admissible if and only if there exists a constant $d \leq L/N$ such that $\bar{v} = V(d)$ and for any $i \in \{1, ..., N\}$, $d = x_{i+1} - x_i$.

Thus each steady-state can be identified by the couple $(\bar{v}, d)$. Since V is an increasing function, the steady-state with highest speed $\bar{v}$ is given by $\bar{v} = V(L/N)$ or equivalently $d = L/N$. We set $\mathbf{v} = (v_1, ..., v_{N+1})$ and $\mathbf{x} = (x_1, ..., x_n)$, and we define $D(\mathbf{v}, \mathbf{x})$ the distance between the solution and a target steady-state $(\bar{v}, d)$ given by

$$D(\mathbf{v}, \mathbf{x}) := \sum_{i=1}^{N+1} |v_i(t) - \bar{v}| + \sum_{i=1}^{N} |x_{i+1}(t) - x_i(t) - d|. \tag{2.5}$$

Our main result is the following

Theorem 2.2. *Let $(\bar{v}, d)$ be an admissible steady-state as in (A1). If $k > 0$ then the system* (2.1), (2.3) *with control feedback* (2.4) *is locally exponentially stable around $(\bar{v}, d)$.*
Moreover, the supremum value of the achievable decay rate is

$$\gamma_{\max} = \min\left(k, \frac{1}{2}\left(\frac{a}{d^2} + b - Re\left(\sqrt{\left(\frac{a}{d^2} + b\right)^2 - 4bV'(d)}\right)\right)\right), \tag{2.6}$$

and for any $\gamma \in (0, \gamma_{\max})$, there exists a characteristic time $\tau > 0$, independent of N, and $\varepsilon > 0$ such that for any initial conditions $(\mathbf{v}_0, \mathbf{x}_0)$ with $D(\mathbf{v}_0, \mathbf{x}_0) \leq \varepsilon$, we have

$$D(\mathbf{v}(t), \mathbf{x}(t)) \leq e^{N\tau} e^{-\gamma t} D(\mathbf{v}_0, \mathbf{x}_0). \tag{2.7}$$

Remark 2.2 (Uniform bounds in N). Note that this result holds for any number of cars N while there is always a single AV. Besides, note that the largest achievable decay rate does not depend on N. Therefore, the value of the gain k to obtain the largest decay rate is also independent of N.

Remark 2.3 (Relaxation time). As it could be expected the total relaxation time $N\tau$ – which can be seen as the characteristic time needed to stabilize the system – is not uniform in N. However, it is proportional to N, which can be seen as an optimal estimate due to the finite speed of propagation of the information in the system.

Remark 2.4 (Basin of attraction). Whereas the the largest accessible decay rate does not depend on N, the size of the basin of attraction likely decreases as the number of cars N increase. We can find a lower bound η on the basin of attraction which satisfies:

$$\eta < \eta_0 e^{-\alpha N}, \tag{2.8}$$

where η_0 and α are constants independent of N. A more detailed estimate is given in Section 3.

We prove Theorem 2.2 in Section 3. The optimality of the condition $k > 0$ in Theorem 2.2 is given by the following Proposition.

Proposition 2.3. *Let $(\bar{v}, d)$ be an admissible steady-state as in (A1). If $k \leq 0$, then the system* (2.1), (2.3) *with control feedback* (2.4) *is not locally asymptotically stable around $(\bar{v}, d)$.*

This is straightforward and proved in detail in Section Section 3.

2.1 Disturbances and proportional integral controllers

Due to disturbances in the AVs speed measurements, there may be a persistent and constant error occurring in the control (2.4). In this case, the disturbance prevents the feedback control from efficiently steering the system to the steady state. To represent this situation, we consider the equation

$$\dot{v}_{N+1} = k(\bar{v} - v_{N+1}) + \delta, \tag{2.9}$$

where $\delta \neq 0$ is a constant unknown disturbance. The convergence of v_{N+1} to $\bar{v}$ would imply $\dot{v}_{N+1} \to 0$ and $\delta = 0$, which is a contradiction. To tackle this issue and recover the exponential stability, a classical approach is used to robustify the control law by using a proportional integral (PI) controller. PI controllers are well-established tools, first used by the Perier brothers [8, Pages 50-51 and figure 231, Plate 26] and mathematized by Minorsky [25]. They have been well studied in the last decades for finite dimensional systems [1, 2]. The idea consists of adding a part proportional to the integration over time of the difference between the state and the target. Its robustness to small perturbations makes this type of controllers more adapted to practical implementations (see [6, 17] for more details). The only price to pay is that the mathematical analysis may sometimes be more complicated [6]. With this in mind, we consider a new control law of the following type:

$$\begin{aligned} u(t) =& k(\bar{v} - v_{N+1}(t)) + k_I Z(t), \\ \dot{Z}(t) =& (\bar{v} - v_{N+1}(t)). \end{aligned} \tag{2.10}$$

The quantity Z is the integral part. The only measurement used by this controller is still the speed of the AV. We show that we can achieve exponential stability also with this controller.

Theorem 2.4. *Let $(\bar{v}, d)$ be an admissible steady-state, if $k > 0$ and $k_I > 0$ then the system (2.1), (2.3) with control feedback (2.10) is locally exponentially stable around $(\bar{v}, d)$.*
Moreover, the supremum value of the achievable decay rate is

$$\gamma_{\max} = \frac{1}{2} \min \left(k - Re\left(\sqrt{k^2 - 4k_I^2} \right), \left(\frac{a}{d^2} + b - Re\left(\sqrt{\left(\frac{a}{d^2} + b \right)^2 - 4bV'(d)} \right) \right) \right), \tag{2.11}$$

and for any $\gamma \in (0, \gamma_{\max})$, there exists a characteristic time $\tau > 0$ independent of N and $\varepsilon > 0$ such that for any initial conditions $(\mathbf{v}_0, \mathbf{x}_0)$ such that $D(\mathbf{v}_0, \mathbf{x}_0) \leq \varepsilon$,

$$D(\mathbf{v}(t), \mathbf{x}(t)) + |Z(t)| \leq e^{N\tau} e^{-\gamma t} \left(D(\mathbf{v}_0, \mathbf{x}_0) + |Z(0)| \right). \tag{2.12}$$

The proof is very similar to the proof of Theorem 2.2 and is given in Appendix A.

We conclude by giving an *Input-to-State Stability* (ISS) estimate with respect to perturbations for a time-varying disturbance $\delta(t)$. In this case, the equation on the control (2.10) is replaced by

$$\begin{aligned} u(t) =& k(\bar{v} - v_{N+1}(t)) + k_I Z(t) + \delta(t), \\ \dot{Z}(t) =& (\bar{v} - v_{N+1}(t)), \end{aligned} \tag{2.13}$$

where $\delta \in L^\infty([0, +\infty), \mathbb{R})$ is the time-varying disturbance. In this case, it is impossible to stabilize a steady-state by designing k and k_I, but we show the following

Theorem 2.5. *Let $(\bar{v}, d)$ be an admissible steady state of the system without disturbance. If $k > 0$ and $k_I > 0$ then there exists $\eta > 0$ such that, for any initial condition $(\mathbf{x}_0, \mathbf{v}_0, Z_0)$ satisfying $D(\mathbf{x}_0, \mathbf{v}_0) < \eta$, and for $\|\delta\|_{L^\infty} < \eta$ the system (2.1), (2.3), (2.13) has a unique solution $(\mathbf{x}, \mathbf{v}) \in C^1([0, +\infty), \mathbf{R}^{2N+2})$ and the following ISS estimate holds for any $\gamma \in (0, \gamma_{\max})$*

$$D(\mathbf{v}(t), \mathbf{x}(t)) + |Z(t)| \leq C_1 e^{N\tau} e^{-\gamma t} \left(D(\mathbf{v}_0, \mathbf{x}_0) + |Z_0| \right) + C_2^N \sup_{s \in [0,t]} |\delta(t)|, \ \forall\ t \geq 0, \tag{2.14}$$

where C_1 and C_2 are constants independent of N.

The notion of ISS, first introduced by Sontag in 1989 for finite dimensional systems [31], measures the resilience of the exponential stability property to unknown perturbations. In other words, it ensures that the exponential stability is not too perturbed by an unknown disturbances, and this "not too much" is quantified in by the ISS gain that is here C_2^N. This notion is more general than the notion of exponential stability and coincide when the disturbance is zero. Looking at this notion is relevant as a system could be exponentially stable but not ISS. From an application perspective this notion is more relevant than the exponential stability as there are always some perturbations in real life. In our case, as $C_2 > 1$ a priori we see, as it could be expected, that the system is more sensitive when the number of car increases.

3 Exponential stability of the steady-state

In this section, we prove Theorem 2.2. Let us consider the system (2.1), (2.3), (2.4), and let $(\bar{v}, d)$ be an admissible steady-state. We rewrite the $2N+1$ components of the system using the following change of variables,

$$\begin{aligned} y_{2p+1} &= x_{p+2} - x_{p+1} - d,\ 0 \le p \le N-1 \\ y_{2p} &= v_{p+1} - v_p,\ 1 \le p \le N \\ y_{2N+1} &= \bar{v} - v_{N+1}. \end{aligned} \tag{3.1}$$

In these variables, the dynamics become

$$\dot{\mathbf{y}} = f(\mathbf{y}, k), \tag{3.2}$$

where f is given by

$$\begin{aligned} f_{2p+1}(y,k) &= y_{2p+2},\ 0 \le p \le N-1 \\ f_{2p}(y,k) &= a\left[\frac{y_{2p+2}}{(d+y_{2p+1})^2} - \frac{y_{2p}}{(d+y_{2p-1})^2}\right] + b[V(d+y_{2p+1}) - V(d+y_{2p-1}) - (y_{2p})],\ 1 \le p \le N-1, \\ f_{2N}(y,k) &= k y_{2N+1} - a\left[\frac{y_{2N}}{(d+y_{2N-1})^2}\right] - b[V(d+y_{2N-1}) + y_{2N} + y_{2N+1} - \bar{v}] \\ f_{2N+1}(y,k) &= -k y_{2N+1}. \end{aligned} \tag{3.3}$$

The stability of the steady-state $(\bar{v}, d)$ for the system (2.1), (2.3), (2.4) is equivalent to the stability of the steady state $\mathbf{y} = 0$ for the system (3.2)–(3.3). Before going any further, observe that, looking at (3.3), for any $p \in \{0, ..., N-2\}$, the dynamics of (y_{2p+1}, y_{2p+2}) only depends on $(y_{2p+1}, y_{2p+2}, y_{2p+3}, y_{2p+4})$, and the dynamics of (y_{2N-1}, y_{2N}) depends only on $(y_{2N-1}, y_{2N}, y_{2N+1})$. This comes from the fact that the acceleration of a vehicle only depends on its state and the state of the car in front. The system has therefore a cascade structure, that we will use in the following, and the Jacobian matrix $\partial_y f(\mathbf{0}, k)$ writes

$$\partial_y f(\mathbf{0}, k) = \begin{pmatrix} A_1 & B_1 & 0 & ... & 0 & \\ 0 & A_1 & B_1 & 0 & ... & \\ ... & ... & ... & ... & ... & \\ 0 & ... & 0 & A_1 & B_1 & 0 \\ 0 & ... & 0 & 0 & A_1 & \begin{pmatrix} 0 \\ k-b \end{pmatrix} \\ 0 & ... & 0 & 0 & 0 & -k \end{pmatrix}, \tag{3.4}$$

where A_1 and B_1 are 2×2 block matrices given by

$$\begin{aligned} A_1 &= \begin{pmatrix} 0 & 1 \\ -bV'(d) & -(\frac{a}{d^2} + b) \end{pmatrix}, \\ B_1 &= \begin{pmatrix} 0 & 0 \\ bV'(d) & \frac{a}{d^2} \end{pmatrix}. \end{aligned} \tag{3.5}$$

Note that A_1 has eigenvalues λ_1 and λ_2 given by

$$\begin{aligned}\lambda_1 &= \frac{-(a+bd^2)-\sqrt{(a+bd^2)^2-4bV'(d)d^4}}{2d^2},\\ \lambda_2 &= \frac{-(a+bd^2)+\sqrt{(a+bd^2)^2-4bV'(d)d^4}}{2d^2}.\end{aligned} \tag{3.6}$$

Here $\sqrt{z}$ refers to $i\sqrt{|z|}$ when $z<0$. Therefore, A_1 is diagonalizable as long as $(a+bd^2)^2 \neq 4bV'(d)d^4$. We assume this for now. In the special case where $(a+bd^2)^2 = 4bV'(d)d^4$ the same result would still hold by trigonalizing the matrix A_1 in $\mathbb{C}$ instead of diagonalizing it. Then there exists S_1 such that

$$S_1^{-1}A_1S_1 = \begin{pmatrix}\lambda_1 & 0\\ 0 & \lambda_2\end{pmatrix} =: \Lambda_1. \tag{3.7}$$

We define now the matrix of change of variables S by

$$S = \begin{pmatrix} S_1 & 0 & 0 & ... & 0 & \\ 0 & S_1 & 0 & ... & 0 & \\ ... & ... & ... & ... & ... & 0\\ 0 & ... & 0 & 0 & S_1 & 0\\ 0 & ... & 0 & 0 & 0 & 1\end{pmatrix}. \tag{3.8}$$

We have

$$S^{-1}\partial_y f(\mathbf{0},k)S = \begin{pmatrix} \Lambda_1 & B_2 & 0 & ... & 0 & \\ 0 & \Lambda_1 & B_2 & 0 & ... & \\ ... & ... & ... & ... & ... & \\ 0 & ... & 0 & \Lambda_1 & B_2 & 0\\ 0 & ... & 0 & 0 & \Lambda_1 & \begin{pmatrix}c_1\\ c_2\end{pmatrix}\\ 0 & ... & 0 & 0 & 0 & -k\end{pmatrix}, \tag{3.9}$$

where B_2 is a 2×2 block matrix and c_1, c_2 are two real numbers. As Λ_1 is diagonal, $S^{-1}\partial_y f(\mathbf{0},k)S$ is triangular, which implies that its only eigenvalues are λ_1, and λ_2 and $-k$. From the change of variables, $\partial_y f(\mathbf{0},k)$ has the same eigenvalues. As $V'>0$, λ_1 and λ_2 have both negative real parts. This implies that, for any $k>0$, the linearized system

$$\dot{\mathbf{z}} = \partial_y f(\mathbf{0},k)\mathbf{z} \tag{3.10}$$

is exponentially stable and therefore the nonlinear system (3.2) is locally exponentially stable [5, Theorem 10.10], which means that $(\bar{v},d)$ is a locally exponentially stable steady-state for the original system (2.1), (2.3), (2.4).

Estimation of the decay rate To obtain the decay rate, we look again at the linearized system (3.10). Using Jordan-Chevalley decomposition, there exist matrices S_2, D and L, such that $\partial_y f(\mathbf{0},k) = D+L$, D and L commute, L is nilpotent of order N and

$$S_2^{-1}DS_2 = \Lambda_2, \tag{3.11}$$

where Λ_2 is the diagonal matrix $\mathrm{diag}(\Lambda_1,....,\Lambda_1,-k)$. We denote $L_2 = S_2^{-1}LS_2$, which is still a nilpotent matrix of order N. From this decomposition, the solution $\mathbf{z}$ of the system (3.10) is

$$\mathbf{z}(t) = S_2 e^{\Lambda_2 t}\left(\sum_{i=0}^{N-1}\frac{(L_2t)^i}{i!}\right)S_2^{-1}\mathbf{z}(0). \tag{3.12}$$

Therefore, as $0>\mathrm{Re}\lambda_2>\mathrm{Re}\lambda_1$, for any $\varepsilon>0$, $\Lambda_2+(\min(k,|\lambda_2|)-\varepsilon)Id$ is still diagonal and its eigenvalues still have negative real parts. The largest real parts of its eigenvalue is $-\varepsilon$. This implies that

$$C_1 := \sup_{t\in[0,+\infty)}\left|S_2 e^{(\Lambda_2+(\min(k,|\lambda_2|)-\varepsilon)Id)t}S_2^{-1}\left(\sum_{i=0}^{N-1}\frac{(Lt)^i}{i!}\right)\right| < +\infty, \tag{3.13}$$

and together with (3.10), we get

$$|\mathbf{z}(t)| \leq C_1 e^{-(\min(k,|\lambda_2|)-\varepsilon)t}|\mathbf{z}(0)|. \tag{3.14}$$

We show next that the total relaxation time is linear in N, or in other words, that there exists a characteristic time τ independent of N such that $C_1 \leq e^{N\tau}$.

Estimation of relaxation time One approach could be to estimate C_1 by carefully studying how L and S_2 are constructed in the Jordan-Chevalley decomposition, using the Chinese remainder theorem. However, we detail here a more intuitive approach, linked to the cascade structure of the system. The idea is the following: we will consider each 2×2 block corresponding to a vehicle as a system with a dynamic depending on itself and some external inputs that are given by the vehicle in front. For each of these blocks, we provide an Input to State Stability estimate with respect to these external inputs. Finally, using the exponential stability of the AV trajectory, we can recover the exponential stability of the entire system with an explicit estimate on the relaxation time. Let us now consider the following system

$$\frac{d}{dt}\begin{pmatrix} q_1 \\ q_2 \end{pmatrix} = \Lambda_1 \begin{pmatrix} q_1 \\ q_2 \end{pmatrix} + B_2 \begin{pmatrix} w_1 \\ w_2 \end{pmatrix}. \tag{3.15}$$

As the eigenvalues of Λ_1 are strictly negative, the solution $\mathbf{q} = (q_1, q_2)^T$ of this system satisfies the following ISS estimate

$$\begin{aligned} |\mathbf{q}(t)| &\leq |\mathbf{q}(0)|e^{-\mathrm{Re}(|\lambda_2|)t} + \int_0^t \left| e^{\Lambda(t-s)} B_2 \mathbf{w}(s) \right| ds \\ &\leq |\mathbf{q}(0)|e^{-\mathrm{Re}(|\lambda_2|)t} + 2\|B_2\|_\infty \int_0^t e^{-|\mathrm{Re}(\lambda_2)|(t-s)} \left|\mathbf{w}(s)\right| ds, \ \forall\, t \geq 0, \end{aligned} \tag{3.16}$$

where $\mathbf{w} = (w_1, w_2)^T$. Let us now set $\gamma_{\max} := \min(k, |\mathrm{Re}(\lambda_2)|)$, which coincide with the definition given in Theorem 2.2. As $\gamma_{\max} \leq |\mathrm{Re}(\lambda_2)|$, (3.16) implies in particular that for any $t \geq 0$,

$$|\mathbf{q}(s)|e^{\gamma_{\max} t} \leq |\mathbf{q}(0)| + 2\|B_2\|_\infty \int_0^t e^{\gamma_{\max} s} \left|\mathbf{w}(s)\right| ds. \tag{3.17}$$

This is the estimate that we will use in the following. Let us come back to the system (3.10) and denote $\xi = S^{-1}\mathbf{z}$, where S is the matrix of change of variables given by (3.8). From (3.10), ξ is solution to

$$\dot{\xi} = \begin{pmatrix} \Lambda_1 & B_2 & 0 & ... & 0 & \\ 0 & \Lambda_1 & B_2 & 0 & ... & \\ ... & ... & ... & ... & ... & \\ 0 & ... & 0 & \Lambda_1 & B_2 & 0 \\ 0 & ... & 0 & 0 & \Lambda_1 & \begin{pmatrix} c_1 \\ c_2 \end{pmatrix} \\ 0 & ... & 0 & 0 & 0 & -k \end{pmatrix} \xi. \tag{3.18}$$

Therefore, for any $j \in \{0, ..., N-2\}$, the function $(\xi_{2j+1}, \xi_{2j+2})^T$ is solution to (3.15) with disturbances $\mathbf{w} = (\xi_{2(j+1)+1}, \xi_{2(j+1)+2})^T$. From (3.17),

$$\begin{aligned} e^{\gamma_{\max} t}|(\xi_{2j+1}(t), \xi_{2j+2}(t))^T| &\leq |(\xi_{2j+1}(0), \xi_{2j+2}(0))^T| \\ &+ 2\|B_2\|_\infty \int_0^t e^{\gamma_{\max} s} \left|(\xi_{2(j+1)+1}(s), \xi_{2(j+1)+2}(s))^T\right| ds. \end{aligned} \tag{3.19}$$

By iterating, we are in position to obtain an estimate on $(\xi_{2j+1}(t), \xi_{2j+2}(t))^T$ for any $i \in \{0, ..., N-2\}$ as a function only of the initial conditions and $(\xi_{2N-1}(t), \xi_{2N}(t))^T$. Thus, we would like to have an estimate on $(\xi_{2N-1}(t), \xi_{2N}(t))$. From (3.18), $(\xi_{2N-1}, \xi_{2N})^T$ is solution to the following system

$$\frac{d}{dt}\begin{pmatrix} \xi_{2N-1} \\ \xi_{2N} \end{pmatrix} = \Lambda_1 \begin{pmatrix} \xi_{2N-1} \\ \xi_{2N} \end{pmatrix} + \begin{pmatrix} c_1 \\ c_2 \end{pmatrix} \xi_{2N+1}. \tag{3.20}$$

Reasoning as above, we get

$$e^{\gamma_{\max} t}\,|(\xi_{2N-1}(t),\xi_{2N}(t))| \le \left|(\xi_{2N-1}(0),\xi_{2N}(0))^T\right| + \max(|c_1|,|c_2|)\int_0^t e^{\gamma_{\max} s}|\xi_{2N+1}(s)|ds. \tag{3.21}$$

From (3.8), $\dot{\xi}_{2N+1} = -k\xi_{2N+1}$, thus, for any $0 \le s \le t$, as $\gamma_{\max} \le k$,

$$|\xi_{2N+1}(t)|e^{\gamma_{\max} t} \le |\xi_{2N+1}(0)|. \tag{3.22}$$

We can now back propagate the exponential stability of ξ_{2N+1} using the ISS estimates (3.19) and (3.21). By recursion, the following holds for $j \in \{0,...,N-1\}$,

$$\begin{aligned} e^{\gamma_{\max} t}|(\xi_{2j+1}(t),\xi_{2j+2}(t))^T| \le &\sum_{i=j}^{N-1} \frac{(2\|B_2\|_\infty t)^{i-j}}{(i-j)!}|(\xi_{2i+1}(0),\xi_{2i+2}(0))^T| \\ &+ \frac{(2\|B_2\|_\infty t)^{(N-1)-j}}{(N-1-j)!}\max(|c_1|,|c_2|)\frac{t}{(N-j)}|\xi_{2N+1}(0)|. \end{aligned} \tag{3.23}$$

Indeed, for $j = N-1$, this comes directly from (3.21) and (3.22). Assuming (3.23) is true for $j \in \{1,...,N-1\}$, then for $(j-1)$, we have, from(3.19),

$$\begin{aligned} e^{-\gamma_{\max} t}|(\xi_{2(j-1)+1}(t),\xi_{2(j-1)+2}(t))^T| &\le |(\xi_{2(j-1)+1}(0),\xi_{2(j-1)+2}(0))^T| \\ &+ 2\|B_2\|_\infty \int_0^t \sum_{i=j}^{N-1} \frac{(2\|B_2\|_\infty s)^{i-j}}{(i-j)!}|(\xi_{2i+1}(0),\xi_{2i+2}(0))^T|ds \\ &+ 2\|B_2\|_\infty \int_0^t \frac{(2\|B_2\|_\infty s)^{(N-1)-j}}{(N-1-j)!}\max(|c_1|,|c_2|)\frac{s}{(N-j)}|\xi_{2N+1}(0)|ds \\ &\le \sum_{i=(j-1)}^{N-1} \frac{(2\|B_2\|_\infty t)^{i-(j-1)}}{(i-(j-1))!}|(\xi_{2i+1}(0),\xi_{2i+2}(0))^T| \\ &+ \frac{(2\|B_2\|_\infty t)^{(N-1)-(j-1)}}{(N-j)!}\max(|c_1|,|c_2|)\frac{t}{(N-(j-1))}|\xi_{2N+1}(0)|, \end{aligned} \tag{3.24}$$

which is exactly (3.23). Summing this estimate for $j \in \{0,...,N-1\}$, we have

$$\begin{aligned} \left(|\xi_{2N+1}(t)| + \sum_{j=0}^{N-1}|(\xi_{2j+1}(t),\xi_{2j+2}(t))^T|\right)e^{\gamma_{\max} t} &\le \sum_{j=0}^{N-1}\sum_{i=j}^{N-1} \frac{(2\|B_2\|_\infty t)^{i-j}}{(i-j)!}|(\xi_{2i+1}(0),\xi_{2i+2}(0))^T| \\ &+ \left(1 + \sum_{j=0}^{N-1}\frac{(2\|B_2\|_\infty t)^{(N-1)-j}}{(N-1-j)!}\max(|c_1|,|c_2|)\frac{t}{(N-j)}\right)|\xi_{2N+1}(0)| \\ &\le \sum_{i=0}^{N}|(\xi_{2i+1}(0),\xi_{2i+2}(0))^T|\left(\sum_{j=0}^{i}\frac{(2\|B_2\|_\infty t)^j}{j!}\right) \\ &+ \sum_{j=0}^{N}\frac{(\max(2\|B_2\|_\infty,|c_1|,|c_2|)t)^j}{j!}|\xi_{2N+1}(0)| \\ &\le \left(|\xi_{2N+1}(0)| + \sum_{i=0}^{N}|(\xi_{2i+1}(0),\xi_{2i+2}(0))^T|\right) \\ &\quad\times\left(\sum_{j=0}^{N}\frac{(\max(2\|B_2\|_\infty,|c_1|,|c_2|)t)^j}{j!}\right). \end{aligned} \tag{3.25}$$

To conclude, let us now set $\gamma \in (0, \gamma_{\max})$, $\varepsilon = \gamma_{\max} - \gamma > 0$, and $C_1 := 2\max(\|B_2\|_\infty, |c_1|, |c_2|) > 0$. We define $g_j(t) = \frac{C_1^j t^j}{j!} e^{-\varepsilon t}$,

$$g_j'(t) = \frac{C_1^j}{j!}(j - \varepsilon t) t^{j-1} e^{-\varepsilon t}, \ \forall\, j \in \{1, ..., N\} \tag{3.26}$$

so that g_j is minimum for $t = j/\varepsilon$. Thus,

$$e^{-\varepsilon t} \left| \sum_{j=0}^{N} \frac{(2\max(\|B_2\|_\infty, |c_1|, |c_2|)t)^j}{j!} \right| \leq 1 + \sum_{j=1}^{N} \frac{C_1^j j^j}{j! \varepsilon^j} e^{-j}. \tag{3.27}$$

From the Stirling formula, $j! \sim \sqrt{2\pi j}(j/e)^j$ which implies that there exists a numerical constant C_0 independent of N, j and the system, such that

$$\sup_{t \in [0, +\infty)} \left| e^{-\varepsilon t} \sum_{j=0}^{N} \frac{(2\max(\|B_2\|_\infty, |c_1|, |c_2|)t)^j}{j!} \right| \leq 1 + C_0 \sum_{j=1}^{N} \frac{1}{\sqrt{2\pi j}} \left(\frac{C_1}{\varepsilon} \right)^j \leq C_0 e^{\tau N} \tag{3.28}$$

where $\tau = \ln(C_1/\varepsilon) = \ln(2\max(\|B_2\|_\infty, |c_1|, |c_2|)/(\gamma_{\max} - \gamma))$. Using this in (3.25), we get

$$\left(|\xi_{2N+1}(t)| + \sum_{j=0}^{N-1} |(\xi_{2j+1}(t), \xi_{2j+2}(t))^T| \right) \leq C_0 e^{\tau N} e^{-\gamma t} \left(|\xi_{2N+1}(0)| + \sum_{i=0}^{N} |(\xi_{2i+1}(0), \xi_{2i+2}(0))^T| \right). \tag{3.29}$$

Using the inverse change of variable $\mathbf{z} = S\xi$, there exists $C_S > 0$ depending only on S such that

$$|\mathbf{z}(t)| \leq C_S e^{\tau N} e^{-\gamma t} |\mathbf{z}(0)|. \tag{3.30}$$

From (3.8) and (3.7), B_2, c_1 and c_2 are independent of N, which implies that C_S and τ is independent of N as well. This is true for the linear system for any $\gamma < \gamma_{\max}$, therefore locally also for the nonlinear system (3.2), (3.3), and, finally, for the original system (2.1), (2.3), (2.4).

Estimation of the basin of attraction Let us complete the analysis by giving an estimate of the basin of attraction. Fix $T > 0$ and consider the nonlinear system (3.2), (3.3) on $[0, T]$. Using the change of variables $\xi = S^{-1}\mathbf{y}$, we get the nonlinear system

$$\dot{\xi} = g(\xi), \tag{3.31}$$

where $\partial_\xi g(0)$ is the triangular matrix given in (3.18). We assume now that $|\xi(0)| < \eta$ where η will be the bound on the basin of attraction of ξ will be chosen later on. Our goal will be first to show that there exists a lower bound for the basin of attraction $\eta = \eta_0^N$, where η_0 is a constant that depends on the final time T but not on N. Of course it would not be enough to stop here as η_0 could go to 0 where T goes to infinity and therefore there would be no uniform bound in time. Therefore, we will then show how to extend this to get a bound $\eta = \eta_0^N$ where η_0 do not depend on T and such that the stability also holds on $[0, +\infty)$.

a) Existence of trajectories for the nonlinear system
First of all, we need to show that for such $\eta = \eta_0^N$, the nonlinear system (3.31) (or equivalently (3.2), (3.3)) is well-posed on $[0, T]$ for any initial condition $|\xi(0)| < \eta$. Since f still has a cascade structure and is C^2, we now have for any $j \in \{0, ..., N-1\}$

$$\frac{d}{dt} \begin{pmatrix} \xi_{2i+1} \\ \xi_{2i+2} \end{pmatrix} = \Lambda_1 \begin{pmatrix} \xi_{2i+1} \\ \xi_{2i+2} \end{pmatrix} + B_2 \begin{pmatrix} \xi_{2(i+1)+1} \\ \xi_{2(i+1)+2} \end{pmatrix} + g\left(\xi_{2i+1}, \xi_{2i+2}, \xi_{2i+3}, \xi_{2i+4}\right), \tag{3.32}$$

where $g(x) = O(|x|^2)$ is independent of N and accounts for the nonlinear part. Let assume from now on that $\xi_{2(i+1)+1}, \xi_{2(i+1)+2}$ exists on $[0, T]$, and that for any $j \geq i + 1$,

$$\sup_{t \in [0,T]} |\xi_{2j+1}, \xi_{2j+2}| \leq \delta, \tag{3.33}$$

where δ does not depend on N and need to be specified. Then exists such a $\delta > 0$, $c(T) > 0$, and $C(T) > 0$ independent of N such that for $\eta < c(T)$, ξ_{2i+1}, ξ_{2i+2} exists on $[0,T]$ and

$$\sup_{s\in[0,T]} |\xi_{2i+1}(t), \xi_{2i+2}(t)| \leq C(T)(|\xi_{2i+1}(0), \xi_{2i+2}(0)| + \sup_{s\in[0,T]} (|\xi_{2(i+1)+1}, \xi_{2(i+1)+2}|)), \tag{3.34}$$

on $[0,T]$. This consideration encourages us to start with ξ_{2N+1} and then to show the existence backward to smaller indices up to y_1. For ξ_{2N+1}, we have

$$\dot{\xi}_{2N+1} = -k\xi_{2N+1}, \tag{3.35}$$

thus ξ_{2n+1} trivially exists on $[0,T]$, without any constraint on η and

$$\sup_{[0,T]} |\xi_{2N+1}(t)| \leq |\xi_{2N+1}(0)|. \tag{3.36}$$

Let us look at ξ_{2N}, ξ_{2N-1}. From (3.2) and the definition of S given by (3.8) (we recall that $\xi = S^{-1}\mathbf{y}$), there exists $\eta_1(T) > 0$ and $C_1(T)$ (independent of N) such that, if $|\xi_{2N}(0), \xi_{2N-1}(0)| < \eta_1(T)$

$$\begin{aligned}\sup_{s\in[0,T]} |\xi_{2N-1}(s), \xi_{2N}(s)| &\leq C_1(T)(|\xi_{2N-1}(0), \xi_{2N}(0)| + \sup_{s\in[0,T]} |\xi_{2N}(s)|), \\ &\leq C_1(T)(|\xi_{2N-1}(0), \xi_{2N}(0)| + |\xi_{2N+1}(0)|).\end{aligned} \tag{3.37}$$

We would now like to use (3.34) by induction together with (3.37) to get the trajectories and bound their norm. To do so, assume that

$$\eta \leq \min\left(\delta\left(C(T)^{(N-1)}C_1(T) + \sum_{j=0}^{N-2} C(T)^{j+1}\right)^{-1}, c(T)\right), \tag{3.38}$$

then we claim that for any $i \in \{1, ..., N-1\}$, (ξ_{2i+1}, ξ_{2i+2}) exists, and

$$\begin{aligned}\sup_{[0,T]} |\xi_{2i+1}(t), \xi_{2i+2}(t)| \leq& C(T)^{(N-1)-i}C_1(T)(|\xi_{2N-1}(0), \xi_{2N}(0)| + |\xi_{2N+1}(0)|)), \\ &+ \sum_{j=i}^{N-2} C(T)^{j+1-i}|\xi_{2j+1}(0), \xi_{2j+2}(0)|.\end{aligned} \tag{3.39}$$

Indeed, for $i = N-1$, this holds thanks to (3.37) and (3.38). For $i \in \{0, ..., N-2\}$, if the claim is true for $i+1$, then from the assumption (3.38) on η and (3.39), (3.33) holds and $\eta < c(T)$. Thus, from (3.34), (ξ_{2i+1}, ξ_{2i+2}) exists on $[0,T]$ and

$$\begin{aligned}&\sup_{s\in[0,T]} |\xi_{2i+1}(t), \xi_{2i+2}(t)| \leq C(T)(|\xi_{2i+1}(0), \xi_{2i+2}(0)| + \sup_{s\in[0,T]} (|\xi_{2(i+1)+1}, \xi_{2(i+1)+2}|)), \\ &\leq C(T)\left((|\xi_{2i+1}(0), \xi_{2i+2}(0)| + C(T)^{(N-1)-i-1}C_1(T)(|\xi_{2N-1}(0), \xi_{2N}(0)| + |\xi_{2N+1}(0)|)\right) \\ &+ \sum_{j=i}^{N-2} C(T)^{j+1-i}|\xi_{2j+1}(0), \xi_{2j+2}(0)|\Bigg) \\ &\leq C(T)^{(N-1)-i}C_1(T)(|\xi_{2N-1}(0), \xi_{2N}(0)| + |\xi_{2N+1}(0)|) \\ &+ \sum_{j=i}^{N-2} C(T)^{j+1-i}|\xi_{2j+1}(0), \xi_{2j+2}(0)|,\end{aligned} \tag{3.40}$$

which ends the induction.

b) Bounds on the basin of attraction on $[0,T]$

Let us now show the bound on the basin of attraction. From (3.32), as there exists $C_g > 0$ such that $|g(x)| \leq C_g|x|^2$, similarly as before,

$$\begin{aligned} e^{|\mathrm{Re}(\lambda_2)|t}\left|\xi_{2i+1}(t),\xi_{2i+2}(t)\right| &\leq \left|\xi_{2i+1}(0),\xi_{2i+2}(0)\right| \\ &+ 2\|B_2\|_\infty \int_0^t e^{|\mathrm{Re}(\lambda_2)|s}\left|\xi_{2(i+1)+1}(s),\xi_{2(i+1)+2}(s)\right| ds \\ &+ C_g\int_0^t e^{|\mathrm{Re}(\lambda_2)|s}\left|\xi_{2i+1}(s),\xi_{2i+2}(s),\xi_{2i+3}(s),\xi_{2i+4}(s)\right|^2 ds. \end{aligned} \tag{3.41}$$

This implies

$$\begin{aligned} &\sup_{s\in[0,t]}\left(e^{|\mathrm{Re}(\lambda_2)|s}\left|\xi_{2i+1}(s),\xi_{2i+2}(s)\right|\right) - TC_g\sup_{s\in[0,t]}\left(e^{|\mathrm{Re}(\lambda_2)|s}\left|\xi_{2i+1}(s),\xi_{2i+2}(s)\right|^2\right) \\ &\leq \left|\xi_{2i+1}(0),\xi_{2i+2}(0)\right| + 2\max(\|B_2,1\|_\infty)\int_0^t e^{|\mathrm{Re}(\lambda_2)|s}\left|\xi_{2(i+1)+1}(s),\xi_{2(i+1)+2}(s)\right|\left(1+C_g\left|\xi_{2(i+1)+1}(s),\xi_{2(i+1)+2}(s)\right|\right) ds \end{aligned} \tag{3.42}$$

Looking at (3.42), and comparing with the linear case given in (3.19), one directly sees that if we can guarantee for any $i \in \{1,...,N-1\}$,

$$C_g\sup_{s\in[0,T]}\left(\left|\xi_{2i+1}(s),\xi_{2i+2}(s)\right|\right) < \frac{1}{T}, \tag{3.43}$$

then we can perform exactly as in the linear case and back propagate again the exponential stability and obtain for any $\gamma \in (0,\gamma_{\max})$

$$\left|\xi_{2i+1}(t),\xi_{2i+2}(t)\right| \leq C_0' e^{\tau' N}e^{-\gamma t}\left|\xi_{2i+1}(0),\xi_{2i+2}(0)\right|, \tag{3.44}$$

where C_0 and τ' are positive constants independent of N, T and η. So, all that remains to get the basin on attraction on $[0,T]$ is to find η such that (3.43) holds. This comes directly from the estimate (3.39) and gives the following sufficient condition on η,

$$\eta < \min\left(\min(C_gT,\delta)\left(C(T)^{(N-1)}C_1(T) + \sum_{j=0}^{N-2}C(T)^{j+1}\right), c(T)\right). \tag{3.45}$$

Written in a less complicated form, this implies that there exists $\eta_0(T)$ such that $\eta < \eta_0(T)^N$ is a lower bound on the basin of attraction. Right now the exponential decay (3.44) is only valid on $[0,T]$, for T that can be arbitrarily large but η_0 depends also on T. We now show how to extend this to $[0,+\infty)$ and have η_0 independent of T.

c) Extending the bound to $[0,+\infty)$

Let $\alpha \in (0,1)$ and select $T_1 > 0$ large enough such that

$$C_0' e^{\tau' N}e^{-\gamma(1-\alpha)T_1} < 1. \tag{3.46}$$

Note that T_1 depends on α and tends to $+\infty$ as α tends to 1. Let us now assume that $\eta < \eta_0(T_1)^N$, then from (3.44) and (3.46)

$$\left|\xi_{2i+1}(T_1),\xi_{2i+2}(T_1)\right| \leq e^{-\alpha\gamma T_1}\left|\xi_{2i+1}(0),\xi_{2i+2}(0)\right|. \tag{3.47}$$

As the system (3.31) is autonomous, the solution at $t = 2T_1$ is equivalent to the solution at $t = T_1$ with an initial condition $\xi(T_1)$, and this quantity exists as, from (3.47), $|\xi(T_1)| < |\xi(0)| < \eta$. Thus, for any $t \in [T_1, 2T_1]$ as $\alpha < 1$,

$$\begin{aligned} \left|\xi_{2i+1}(t),\xi_{2i+2}(t)\right| &\leq C_0' e^{\tau' N}e^{-\alpha\gamma(t-T_1)}\left|\xi_{2i+1}(T_1),\xi_{2i+2}(T_1)\right| \\ &\leq C_0' e^{\tau' N}e^{-\gamma(t-T_1)}e^{-\alpha\gamma T_1}\left|\xi_{2i+1}(0),\xi_{2i+2}(0)\right| \\ &\leq C_0' e^{\tau' N}e^{-\alpha t}\left|\xi_{2i+1}(0),\xi_{2i+2}(0)\right|. \end{aligned} \tag{3.48}$$

One can do the same on $[nT_1, (n+1)T_1]$. Finally, we have for any $t \in [0, +\infty)$

$$|\xi_{2i+1}(s), \xi_{2i+2}(s)| \leq C_0' e^{\tau' N} e^{-\alpha\gamma t} |\xi_{2i+1}(0), \xi_{2i+2}(0)|. \tag{3.49}$$

As α was chosen arbitrarily in $(0,1)$ and γ was arbitrary in $(0, \gamma_{\max})$, the above equation is true for any $\alpha\gamma \in (0, \gamma_{\max})$. Of course the choice of decay rate $\alpha\gamma$ impacts the choice of C_0 and T_1, and consequently on η_0 and the bound on the basin of attraction η given by η_0^N. This concludes the proof of Theorem 2.2. Note that, while the estimate on the time needed to stabilize the AV is likely to be optimal, this estimate on η, exponential with the number of cars N, is likely to be conservative.

Proof of Proposition 2.3 To prove Proposition 2.3, note that if $k \leq 0$, from (2.3), (2.4) the velocity of the AV v_{N+1} does not converge to $\bar{v}$ if $v_{N+1}(0) \neq 0$. This ends the proof of Proposition 2.3.

4 Numerical Simulations and stabilization of a multilane ring-road

In this section, we provide two sets of simulations. These simulations are obtained by discretizing and solving the system of ODEs with an Runge-Kutta method of order 4. We present a first set of simulations on a single lane ring road to illustrate our theoretical results. Then, a second set where we apply our controllers to a multilane setting.

4.1 Single-lane ring road

In Figure 1, we show the final average speed of the system with different vehicle densities, when we apply the controller and when no controller is applied (only regular vehicles). In addition to the Bando-FtL model, the vehicles have a maximum acceleration ($2.5m.s^{-2}$) and maximum deceleration ($4m.s^{-2}$). The average speed of the system without controller is represented in red. The average speed with controller in green. And the uniform flow velocity in blue. The speed represented is averaged over the vehicles and over the 200 last seconds, in order to account for the speed variance due to stop and go waves in the uncontrolled case. The road length is $L = 260m$, $a = 20$, $b = 0.5$, and the optimal velocity $V(h)$ is given by

$$V(h) = V_{\max} \frac{\tanh(\frac{h - l_v}{d_0} - 2) + \tanh(2)}{1 + \tanh(2)}, \tag{4.1}$$

where h is the headway between two vehicles, l_v is the length of a vehicle and $d_0 = 2.5$ is a characteristic length. This optimal velocity is commonly used in the literature and one can check that is has the properties expected in Section 2. At $t = 0$, all the vehicles are in the uniform steady-state $x_{i+1} - x_i = L/N$ and $v_i = V(L/N)$ for any $i \in \{1, ..., N\}$ (with the slight abuse of notation $N + 1 = 1$).

We remark that the controlled system always reaches the optimal steady state, while the uncontrolled system never does. Interestingly, we also see in Figure 1 that, above a certain density, the system has a higher throughput with stop and go waves than in uniform flow. However, from an energy consumption point of view, the uniform flow is a much better regime as can be seen in Figure 2 (upper left). The energy model used is the PΔP model derived in [30].

Smoothing existing stop-and-go waves The theoretical results we obtained deal with local stability. This is typically enough when the aim is to prevent the emergence of stop and go waves from a state close to a steady-state. However, if large stop and go waves are already present in the system, such results may fail because the perturbations are already too large. Nevertheless, in the following simulations, we show that even with large perturbations the stabilization seems to be effective. The most problematic point being that our control law may induce AV to crash with the car in front if nothing is done. To avoid this, we complement our control strategy with two safety mechanisms:

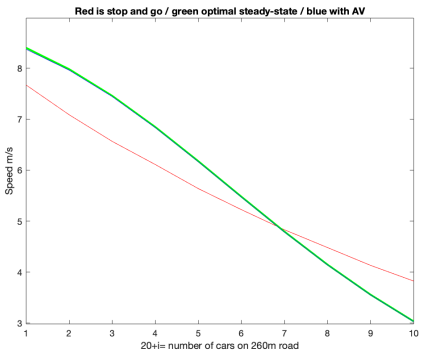

Figure 1: Comparison of terminal velocity with respect to number of cars on the road. Uncontrolled case is in red, controlled in blue and the reference uniform steady-state in green.

- Quasi-stationary target speed. Instead of stabilizing directly the optimal steady-state speed $(\bar{v}, L/(N+1))$, which might impose the AV to be too fast compared to the other cars, we first stabilize to another, slower, steady-state $(\bar{v}_d, d)$ and then increase gradually the speed $\bar{v}_d$ until reaching $\bar{v}$. Hence, the AV is following a continuous path of steady states as described in [5, Chapter 7]. Note that this continuous path of steady states is only possible because of the presence of the AV and does not exist in the uncontrolled case. The control law becomes

$$\begin{aligned} u(t) &= k(\bar{v}_d(t) - v_{N+1}) + Z, \\ \dot{Z} &= (\bar{v}_d(t) - v_{N+1}), \end{aligned} \tag{4.2}$$

  where

$$\begin{cases} v_d(t) = v_{\min} + (\bar{v} - v_{\min})\dfrac{t}{\bar{t}}, & \text{for } t \in [0, \bar{t}] \\ v_d(t) = \bar{v}, & \text{for } t \geq \bar{t}. \end{cases} \tag{4.3}$$

  When using the proportional control of Theorem 2.2, $v_d'(t)/v(t)$ has to be small compared to k to ensure quasi-stationarity, but this assumption is not needed when using the PI controller and when v_d' is kept constant. The reason behind this is that v_d' plays the same role as a disturbance in the control law (see next paragraph).

- When the AV is too close from the vehicle in front, the control law is changed to

$$u(t) = -k(v_{N+1} - \min(v_{\text{leader}}, \bar{v}_d(t))). \tag{4.4}$$

This control law forces the AV to decelerate when the headway is too small and its speed too high. Let us emphasize that these mechanisms are only here to deal with large perturbations and the local asymptotic stability of the system (2.1), (2.3), with the control feedback (2.4) or (2.10) complemented with these two safety mechanisms can be deduced from Theorem 2.2. Indeed, when looking at the local asymptotic stability, the control law is never changed to (4.4). Applying [5, Chapter 7], [23] to the control described in Theorem 2.2 with (4.2) shows that the system still converges eventually to $\bar{v}$ if $v_d'(t)/v(t)$ is small compared to k. When using the PI controller described by Theorem 2.4 with v_d' constant, it is even easier: one can define $Z_1 = Z - v_d'$ and (A.1) still holds with $y_{2N+2} = Z_1$ instead of Z, so the analysis remains exactly the same.

We now consider a situation where we start with human-driven cars and we see the formation of stop and go waves inducing large perturbations. The parameters and the length of the road are identical as in previous simulations and the number of cars is 26. At $t = 1000s$, we turn on the AV control. The average speed of the vehicles and the speed variance at each time are depicted in Figure 2 (lower left right and upper right respectively). Notice the sharp drop of the speed variance as soon as the AV control is turned on. The optimal steady-state speed is highlighted with dashed green line. The speed variance quickly converges near

0 in less than 100 s, while the system finally converges to the optimal steady-state after around 800 s. Notice the drop in the average speed when the AV control is turned on, before the average speed increases slowly up to the target speed. This results from the quasi-stationary target speed strategy.
More generally, a temporary speed drop is unavoidable when the system starts with stop-and-go waves. Indeed, to avoid crashing into the front car, the AV cannot go faster than if it was acting as a human-driven vehicle at all times. Therefore, the only possible strategy is to use a lower speed and then aim for the target steady-state speed, as the natural speed of human-driven cars increases. This is illustrated in Figure 2 (lower left).

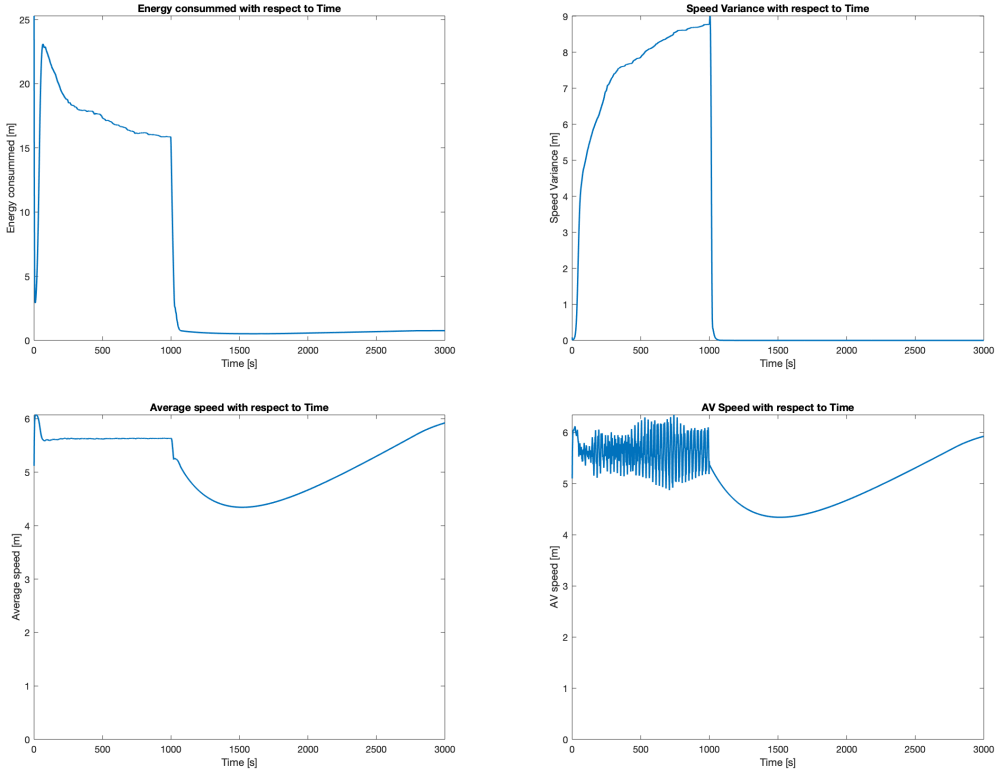

Figure 2: **Upper left:** Average energy consumption per meter travelled with respect to time. **Upper right:** Speed variance on the road with respect to time. **Lower left:** Speed of the AV with respect to time. **Lower right:** Average velocity on the road with respect to time. Control start at $t = 1000s$.

4.2 Multilane ring-road

In this subsection, we apply our controller to a three-lane ring road. This requires to add a lane changing condition to the dynamics. We consider a lane changing condition taken from [22]: a vehicle changes lane if and only if it has an incentive in acceleration and if its lane change does not cause excessive braking (for him or for the vehicle that would be right behind him).Mathematically this translates as follows:

A regular vehicle in a lane i changes by a lateral move to a neighboring lane $j \in \{i-1, i+1\} \cap \{1, ..., J\}$ if and only if

$$\tilde{a}_i^j > a_i + \Delta \tag{4.5}$$

$$\tilde{a}_i^j > -\Delta, \;\; \tilde{a}_{\text{fol}}^j(i) > -\Delta \tag{4.6}$$

where $a_i = \dot{v}_i$ is the acceleration of the i-th vehicle given by (3.2), while $\tilde{a}_i^j$ is the expected acceleration in the new lane. That is, $\tilde{a}_i^j$ is the acceleration that the i-th vehicle would have if it were in lane j instead. Finally $\tilde{a}_{fol}^j(i)$ is the expected acceleration of the follower of the i-th vehicle in lane j, that is, the acceleration that the vehicle right behind the i-th vehicle would have if the i-th vehicle was in lane j instead.

The (longitudinal) control law for the AV is the same as before with the target speed $\bar{v} = V(L/N_i)$, where L_i is the length of the lane in which the AV is and $N_i(t)$ the number of vehicles is this lane. The only difference with the previous subsection is that $\bar{v}$ now changes with time at each lane change occur. We also complement this control law with the two safety mechanisms described in the previous subsection to account for large perturbations.

We now design a lateral control for the AV, that is, a lane-changing mechanism for the AV to stabilize the system in all three lanes. Let t_1 and t_2 be time parameters. The AV changes lane at time t if and only if the three following conditions are satisfied:

1. The safety conditions are satisfied;
2. The speed variance in another lane is higher than the average speed variance in the AV's lane averaged on the last t_1 seconds plus a threshold c_1;
3. The AV has not been changing lanes in the last t_2 seconds.

In precise mathematical terms, let us denote $x_{i,j}$ and $v_{i,j}$ the location and velocity of the $i-th$ vehicle in the j lane. Let $j_0 \in \{1, ...J\}$ be the lane where the AV is at time t^-, i_0 be the car number of the AV in this lane, and t_0 be the last time at which the AV has changed lane, with $t_0 = 0$ if the AV never changed lane. The AV changes lane if

1. $t > t_1$ and there exists $j \in \{1, ..., J\} \setminus \{j_0\}$ such that

$$\begin{aligned} &\int_{t-t_1}^{t} \frac{1}{N}\sum_{i=1}^{n} v_{i,j}^2(s) - \frac{1}{N^2}\left(\sum_{i=1}^{n} v_{i,j}(s)\right)^2 ds \\ &\qquad > c_1 + \int_{t-t_1}^{t} \frac{1}{N}\sum_{i=1}^{n} v_{i,j_0}^2(s) - \frac{1}{N^2}\left(\sum_{i=1}^{n} v_{i,j_0}(s)\right)^2 ds; \end{aligned} \tag{4.7}$$

2. $t > t_2 + t_0$;
3. the safety condition (4.6) is satisfied with $i = i_0$ and $j = j_0$.

In Figure 3, we provide an example simulation. We show the speed variance in each lane, the number of vehicles per lane, and the energy consumption with respect to time. In this simulation, the outer lane length is $L_1 = 298m$, the middle lane length is $L_2 = 279m$, and the inner lane length is $L_3 = 260m$. The simulation starts with 25 vehicles per lane and run for $1500s$. At $t = 750s$, we turn the AV on. We can see that turning the AV on quickly stabilizes the entire system despite having a very low penetration rate (around 1.3%). We can also see that the cars are more stable with the AV activated. After the AV turns on at $750s$, the speed variance quickly drops and remains between 0 and 0.5. Also, once the AV is activated, there seems to be less lane changes as well. The energy consumption per distance travelled is obtained from the PΔT model derived in [30] for a combustion engine. This has to be taken with precautions for two reasons: the energy model might not be representative of the reality (no electric vehicles are included, parameters are generic, etc.); the case studied here is a ring-road where the effect of wave can have a huge effect on the energy consumption in practice (see [39]). Nevertheless, we can see qualitatively a decrease in the energy consumption, which seems logical given the strong decrease of speed variance in the system. To confirm these insights, we ran 50 simulations with random initial perturbations and we present in Table 1 the different resulting averaged quantities before and after the activation of the control.

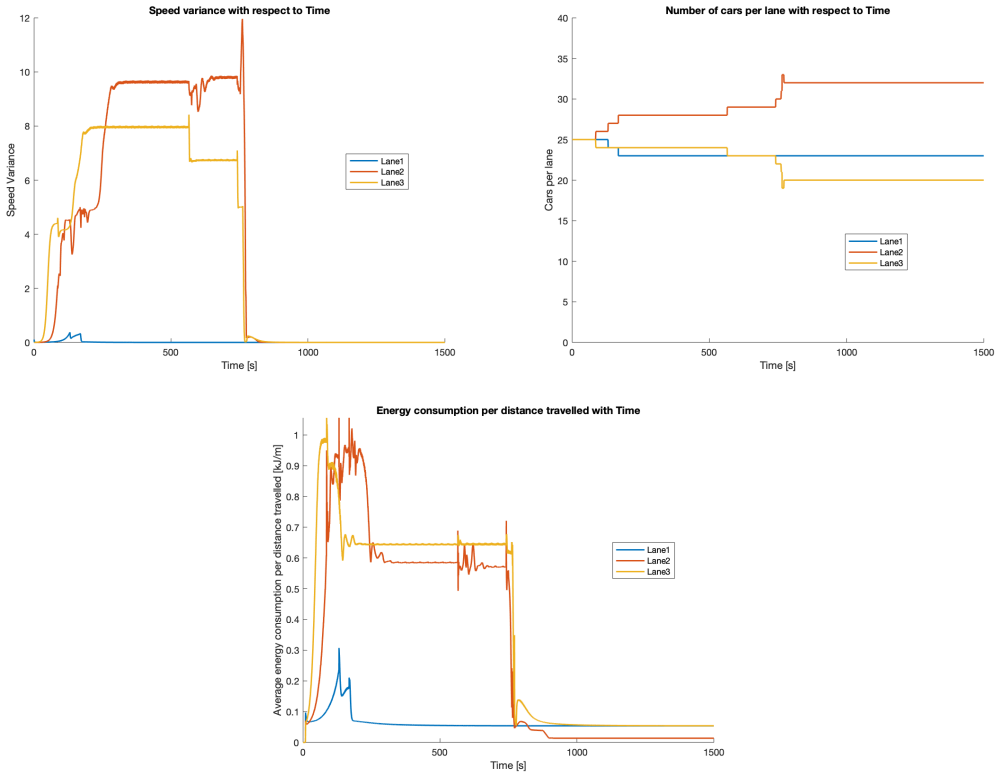

Figure 3: **Left:** Speed variance with respect to time in a three lanes ring-road. **Right:** Number of vehicles per lane with respect to time. **Below:** Energy consumption (PΔP model) per distance travelled with respect to time. Control starts at $t = 750s$.

Acknowledgements

The research of ST was partially supported by Rutgers Global via the International Collaborative Research Grant "Mean field game models for traffic application". BP acknowledges the support of the National Science Foundation under Grants No. CNS-1837481. The research is based upon work supported by the U.S. Department of Energy's Office of Energy Efficiency and Renewable Energy (EERE) under the Vehicle Technologies Office award number CID DE-EE0008872. The views expressed herein do not necessarily represent the views of the U.S. Department of Energy or the United States Government.

Time	$700s$ (before control)	$1500s$ (after control)
Speed variance lane 1 $(m^2.s^{-2})$	2.88	0.55
Speed variance lane 2 $(m^2.s^{-2})$	3.27	0.03
Speed variance lane 3 $(m^2.s^{-2})$	4.59	0.14
Average speed lane 1 $(m.s^{-1})$	7.83	8.46
Average speed lane 2 $(m.s^{-1})$	7.68	7.62
Average speed lane 3 $(m.s^{-1})$	7.18	8.40
Energy consumption per distance lane 1 $(kJ.km^{-1})$	324	98
Energy consumption per distance lane 2 $(kJ.km^{-1})$	295	51
Energy consumption per distance lane 3 $(kJ.km^{-1})$	381	78
Total speed variance $(m^2.s^{-2})$	**3.58**	**0.24**
Total average speed $(m.s^{-1})$	**7.57**	**8.16**
Total energy consumption per distance $(kJ.km^{-1})$	**333**	**76**
Number of lane-change per minute	**1.64**	**0.34**

Table 1: Speed variance, average speed, energy consumption per distance travelled and number of lane-change per minutes before activation of the control ($t = 700s$) and after ($t = 1500s$). Control is activated at $t = 750s$ and all quantities are averaged on 50 simulations. At $t = 0$, each lane has 25 vehicles and the AV is in the middle lane.

A Proportional Integral control

In this appendix, we prove Theorem 2.4 by adapting the proof of Theorem 2.2. Performing the same change of variable (3.1) as previously and setting $y_{2N+2} = Z$ we get (3.2) where

$$\begin{aligned}
f_{2p+1}(y,k) &= y_{2p+2},\ 0 \le p \le N-1 \\
f_{2p}(y,k) &= a\left[\frac{y_{2p+2}}{(d+y_{2p+1})^2} - \frac{y_{2p}}{(d+y_{2p-1})^2}\right] + b[V(d+y_{2p+1}) - V(d+y_{2p-1}) - (y_{2p})],\ 1 \le p \le N-1, \\
f_{2N}(y,k) &= ky_{2N+1} - a\left[\frac{y_{2N}}{(d+y_{2N-1})^2}\right] - b[V(d+y_{2N-1}) + y_{2N} + y_{2N+1} - \bar{v}] \\
f_{2N+1}(y,k) &= -ky_{2N+1} - k_I Z, \\
f_{2N+2}(y,k) &= y_{2N+1},
\end{aligned} \tag{A.1}$$

such that

$$\partial_y f(\mathbf{0},k) = \begin{pmatrix}
A_1 & B_1 & 0 & ... & ... & ... & 0 \\
0 & A_1 & B_1 & 0 & ... & ... & 0 \\
... & ... & ... & ... & ... & ... & ... \\
0 & ... & 0 & A_1 & B_1 & 0 & 0 \\
0 & ... & 0 & 0 & A_1 & \begin{pmatrix} 0 \\ k-b \end{pmatrix} & 0 \\
0 & ... & 0 & 0 & 0 & -k & -k_I \\
0 & ... & 0 & 0 & 0 & 1 & 0
\end{pmatrix}, \tag{A.2}$$

such that redefining S by

$$S = \begin{pmatrix} S_1 & 0 & 0 & ... & ... & ... & 0 \\ 0 & S_1 & 0 & ... & ... & ... & 0 \\ ... & ... & ... & ... & ... & ... & ... \\ 0 & ... & 0 & 0 & S_1 & 0 & 0 \\ 0 & ... & 0 & 0 & 0 & \lambda_3 & \lambda_4 \\ 0 & ... & 0 & 0 & 0 & 1 & 1 \end{pmatrix}, \tag{A.3}$$

where S_1 is given by (3.7), and $\lambda_3 = -(k - \sqrt{k^2 - 4k_I^2})/2$ and $\lambda_4 = -(k + \sqrt{k^2 - 4k_I^2})/2$, we have

$$S^{-1}\partial_y f(\mathbf{0}, k)S = \begin{pmatrix} \Lambda_1 & B_2 & 0 & ... & ... & 0 \\ 0 & \Lambda_1 & B_2 & 0 & ... & 0 \\ ... & ... & ... & ... & ... & ... \\ 0 & ... & 0 & \Lambda_1 & B_2 & 0 \\ 0 & ... & 0 & 0 & \Lambda_1 & B_3 \\ 0 & ... & 0 & 0 & 0 & \Lambda_I \end{pmatrix}, \tag{A.4}$$

where B_3 is a 2×2 block diagonal matrix and Λ_I is given by

$$\Lambda_I := \begin{pmatrix} \lambda_3 & 0 \\ 0 & \lambda_4 \end{pmatrix} = \begin{pmatrix} -\frac{k-\sqrt{k^2-4k_I^2}}{2} & 0 \\ 0 & -\frac{k+\sqrt{k^2-4k_I^2}}{2} \end{pmatrix}. \tag{A.5}$$

As previously, this implies that the only eigenvalues of $\partial_y f(\mathbf{0}, k)$ are λ_1, λ_2, λ_3 and λ_4. Besides, from (A.5) these eigenvalues have all negative real part if and only if $k > 0$ and $k_I > 0$. As in the proof of 2.2, this implies that the system (A.1), (2.3), (2.10) is locally exponentially stable. The analysis of the decay rate and the characteristic time can be done exactly as previously. This ends the proof of Theorem 2.4.

B Input-to-state stability with noise function

In this section, we prove Theorem 2.5. This proof is mainly a variation of the proof of Theorem 2.2. Let us first consider the case of a noise function $\delta \in L^\infty$. The system (2.1), (2.3), (2.10) is still equivalent to the system (3.2), (3.3), with the following change

$$\begin{aligned} \mathbf{y}_{2N+1} &= -k\mathbf{y}_{2N+1} + k_I Z + \delta(t), \\ \dot{Z} &= y_{2N+1}. \end{aligned} \tag{B.1}$$

As previously, we look at the linearized system which can be written

$$\dot{\mathbf{z}} = \partial_y f(\mathbf{0})\mathbf{z} + V_1\delta(t), \tag{B.2}$$

where $\partial_y f(\mathbf{0}$ is given by (A.2) and $V_1 = (0, ..., 0, 1, 0)^T \in \mathbb{R}^n$. We can use once again the change of variable $\xi = S^{-1}\mathbf{y}$, where S is given by (A.3), so that this system becomes

$$\dot{\xi} = \partial_\xi g(\mathbf{0})\xi + S^{-1}V_1\delta(t), \tag{B.3}$$

where $\partial_\xi g(\mathbf{0})$ is given as previously by (3.18). Note that from (A.3), $S^{-1}V_1 = V_1$. Therefore the disturbances still only concerns the previous last equation of the system corresponding to ξ_{2N+1}. As the first equations are same as previously, estimates (3.17), (3.19)–(3.21) still hold, the only difference being (3.22) which now becomes

$$\dot{\xi}_{2N+1}(t) = -k\xi_{2N+1}(t) + \delta(t), \tag{B.4}$$

thus, as $0 < \gamma_{\max} \leq k$,

$$\xi_{2N+1}(t) \leq |\xi_{2N+1}(0)|e^{-\gamma_{\max}t} + e^{-\gamma_{\max}t}\int_0^t e^{\gamma_{\max}s}\delta(s)ds. \tag{B.5}$$

Using (3.21) as previously, we get

$$e^{\gamma_{\max} t}\,|(\xi_{2N-1}(t),\xi_{2N}(t))| \le \left|(\xi_{2N-1}(0),\xi_{2N}(0))^T\right| + \max(|c_1|,|c_2|)\left(t|\xi_{2N+1}(0)| + \frac{e^{\gamma_{\max} s}-1}{\gamma_{\max}} \sup_{s\in[0,t]}|\delta(s)|\right), \tag{B.6}$$

and using (3.19), we get by induction, that for all $i \in \{0,...,N-1\}$,

$$\begin{aligned} e^{\gamma_{\max} t}|(\xi_{2j+1}(t),\xi_{2j+2}(t))^T| \le & \sum_{i=j}^{N-1} \frac{(2\|B_2\|_\infty t)^{i-j}}{(i-j)!}|(\xi_{2i+1}(0),\xi_{2i+2}(0))^T| \\ & + \frac{(2\|B_2\|_\infty t)^{(N-1)-j}}{(N-1-j)!}\max(|c_1|,|c_2|)\frac{t}{(N-j)}|\xi_{2N+1}(0)| \\ & + (2\|B_2\|_\infty)^{(N-1)-j}\max(|c_1|,|c_2|)\left(\frac{e^{\gamma_{\max} t}}{\gamma_{\max}^{N-j}} - \sum_{k=0}^{N-1-j}\frac{t^k}{k!\gamma_{\max}^{N-j-k}}\right)\sup_{s\in[0,t]}|\delta(s)|. \end{aligned} \tag{B.7}$$

Therefore,

$$\begin{aligned} & \left(|\xi_{2N+1}(t)| + \sum_{j=0}^{N-1}|(\xi_{2j+1}(t),\xi_{2j+2}(t))^T|\right)e^{\gamma_{\max} t} \\ & \le \left(|\xi_{2N+1}(0)| + \sum_{i=0}^{N}|(\xi_{2i+1}(0),\xi_{2i+2}(0))^T|\right)\left(\sum_{j=0}^{N}\frac{(\max(2\|B_2\|_\infty,|c_1|,|c_2|)t)^j}{j!}\right) \\ & + e^{\gamma_{\max} t}\sup_{s\in[0,t]}|\delta(s)| + \sum_{j=0}^{N-1}(2\|B_2\|_\infty)^{(N-1)-j}\max(|c_1|,|c_2|)\frac{1}{\gamma_{\max}^{N-j}}\left(e^{\gamma_{\max} t} - \sum_{k=0}^{N-1-j}\frac{(\gamma_{\max} t)^k}{k!}\right)\sup_{s\in[0,t]}|\delta(s)| \\ & \le \left(|\xi_{2N+1}(0)| + \sum_{i=0}^{N}|(\xi_{2i+1}(0),\xi_{2i+2}(0))^T|\right)\left(\sum_{j=0}^{N}\frac{(\max(2\|B_2\|_\infty,|c_1|,|c_2|)t)^j}{j!}\right) \\ & \qquad + e^{\gamma_{\max} t}\sup_{s\in[0,t]}|\delta(s)|\left(1 + \sum_{j=0}^{N-1}\frac{(\max(2\|B_2\|_\infty,|c_1|,|c_2|))^{j+1}}{\gamma_{\max}^{j+1}}\right). \end{aligned} \tag{B.8}$$

We can then proceed exactly as in (3.25)–(3.29), to get, for any $\gamma \in (0,\gamma_{\max})$,

$$\begin{aligned} \left(|\xi_{2N+1}(t)| + \sum_{j=0}^{N-1}|(\xi_{2j+1}(t),\xi_{2j+2}(t))^T|\right) \le & e^{\tau N}e^{-\gamma t}\left(|\xi_{2N+1}(0)| + \sum_{j=0}^{N-1}|(\xi_{2j+1}(0),\xi_{2j+2}(0))^T|\right) \\ & + G_1^N \sup_{[0,t]}|\delta(s)|, \end{aligned} \tag{B.9}$$

where G_1 is a constant gain independent of N. Finally, using the inverse change of variable $\mathbf{y} = S\xi$ and the definition of S given by (A.3), we obtain the ISS estimate (2.14). The extension to the nonlinear provided that η is sufficiently small follows as in Section 3.

References

[1] Karl Johan Åström and Tore Hägglund. PID controllers: theory, design, and tuning, volume 2. Instrument society of America Research Triangle Park, NC, 1995.

[2] Karl Johan Åström and Richard M. Murray. Feedback systems. Princeton University Press, Princeton, NJ, 2008. An introduction for scientists and engineers.

[3] Masako Bando, Katsuya Hasebe, Akihiro Nakayama, Akihiro Shibata, and Yuki Sugiyama. Dynamical model of traffic congestion and numerical simulation. Physical review E, 51(2):1035, 1995.

[4] Georges Bastin and Jean-Michel Coron. Stability and boundary stabilization of 1-D hyperbolic systems, volume 88 of Progress in Nonlinear Differential Equations and their Applications. Birkhäuser/Springer, [Cham], 2016. Subseries in Control.

[5] Jean-Michel Coron. Control and nonlinearity, volume 136 of Mathematical Surveys and Monographs. American Mathematical Society, Providence, RI, 2007.

[6] Jean-Michel Coron and Amaury Hayat. PI controllers for 1-D nonlinear transport equation. IEEE Transactions on Automatic Control, 64(11):4570–4582, 2019.

[7] Shumo Cui, Benjamin Seibold, Raphael Stern, and Daniel B Work. Stabilizing traffic flow via a single autonomous vehicle: Possibilities and limitations. In 2017 IEEE Intelligent Vehicles Symposium (IV), pages 1336–1341. IEEE, 2017.

[8] Riche de Prony. Nouvelle architecture hydraulique, seconde partie. Firmin Didot, Paris, 1796.

[9] Argiris I Delis, Ioannis K Nikolos, and Markos Papageorgiou. Macroscopic traffic flow modeling with adaptive cruise control: Development and numerical solution. Computers & Mathematics with Applications, 70(8):1921–1947, 2015.

[10] Maria Laura Delle Monache, Thibault Liard, Anaïs Rat, Raphael Stern, Rahul Bhadani, Benjamin Seibold, Jonathan Sprinkle, Daniel B Work, and Benedetto Piccoli. Feedback control algorithms for the dissipation of traffic waves with autonomous vehicles. In Computational Intelligence and Optimization Methods for Control Engineering, pages 275–299. Springer, 2019.

[11] Tara E Galovski and Edward B Blanchard. Road rage: a domain for psychological intervention? Aggression and Violent Behavior, 9(2):105–127, 2004.

[12] Mauro Garavello, Paola Goatin, Thibault Liard, and Benedetto Piccoli. A multiscale model for traffic regulation via autonomous vehicles. Journal of Differential Equations, 269(7):6088–6124, 2020.

[13] Denos C Gazis, Robert Herman, and Richard W Rothery. Nonlinear follow-the-leader models of traffic flow. Operations research, 9(4):545–567, 1961.

[14] Xiaoqian Gong, Benedetto Piccoli, and Giuseppe Visconti. Mean-field limit of a hybrid system for multi-lane multi-class traffic. arXiv preprint arXiv:2007.14655, 2020.

[15] Xiaoqian Gong, Benedetto Piccoli, and Giuseppe Visconti. Mean-field of optimal control problems for hybrid model of multilane traffic. IEEE Control Systems Letters, 2020.

[16] Martin Gugat, Michael Herty, Axel Klar, and Günter Leugering. Optimal control for traffic flow networks. Journal of optimization theory and applications, 126(3):589–616, 2005.

[17] Amaury Hayat. PI controllers for the general Saint-Venant equations. January 2019. working paper or preprint.

[18] Andreas Hegyi, Bart De Schutter, and Johannes Hellendoorn. Optimal coordination of variable speed limits to suppress shock waves. IEEE Transactions on intelligent transportation systems, 6(1):102–112, 2005.

[19] Kuang Huang, Xuan Di, Qiang Du, and Xi Chen. Stabilizing traffic via autonomous vehicles: A continuum mean field game approach. In 2019 IEEE Intelligent Transportation Systems Conference (ITSC), pages 3269–3274. IEEE, 2019.

[20] Wen-Long Jin. A kinematic wave theory of lane-changing traffic flow. Transportation research part B: methodological, 44(8-9):1001–1021, 2010.

[21] Nicolas Kardous, Amaury Hayat, Sean T McQuade, Xiaoqian Gong, Sydney Truong, Paige Arnold, Alexandre M Bayen, and Benedetto Piccoli. A rigorous multi-population multi-lane hybrid traffic model and its mean-field limit for dissipation of waves via autonomous vehicles. In Transportation Research Board Conference, 2021.

[22] Arne Kesting, Martin Treiber, and Dirk Helbing. General lane-changing model MOBIL for car-following models. Transportation Research Record, 1999(1):86–94, 2007.

[23] Hassan K. Khalil. Nonlinear systems. Macmillan Publishing Company, New York, 1992.

[24] Jorge A Laval and Carlos F Daganzo. Lane-changing in traffic streams. Transportation Research Part B: Methodological, 40(3):251–264, 2006.

[25] Nicolas Minorsky. Directional stability of automatically steered bodies. Naval Engineers Journal, 32(2), 1922.

[26] Markos Papageorgiou, Habib Hadj-Salem, and F Middelham. Alinea local ramp metering: Summary of field results. Transportation research record, 1603(1):90–98, 1997.

[27] Benedetto Piccoli. Hybrid systems and optimal control. In Proceedings of the 37th IEEE Conference on Decision and Control (Cat. No. 98CH36171), volume 1, pages 13–18. IEEE, 1998.

[28] Hannah Pohlmann and Benjamin Seibold. Simple control options for an vehicle used to dissipate traffic waves. Technical report, 2015.

[29] Rabie A Ramadan and Benjamin Seibold. Traffic flow control and fuel consumption reduction via moving bottlenecks. arXiv preprint arXiv:1702.07995, 2017.

[30] Robin Smit. Development and performance of a new vehicle emissions and fuel consumption software ($p\delta p$) with a high resolution in time and space. Atmospheric pollution research, 4(3):336–345, 2013.

[31] Eduardo D. Sontag. Smooth stabilization implies coprime factorization. IEEE Trans. Automat. Control, 34(4):435–443, 1989.

[32] Eduardo D. Sontag. Input to State Stability: Basic Concepts and Results, pages 163–220. Springer Berlin Heidelberg, Berlin, Heidelberg, 2008.

[33] Raphael E Stern, Shumo Cui, Maria Laura Delle Monache, Rahul Bhadani, Matt Bunting, Miles Churchill, Nathaniel Hamilton, Hannah Pohlmann, Fangyu Wu, Benedetto Piccoli, et al. Dissipation of stop-and-go waves via control of autonomous vehicles: Field experiments. Transportation Research Part C: Emerging Technologies, 89:205–221, 2018.

[34] Yuki Sugiyama, Minoru Fukui, Macoto Kikuchi, Katsuya Hasebe, Akihiro Nakayama, Katsuhiro Nishinari, Shin-ichi Tadaki, and Satoshi Yukawa. Traffic jams without bottlenecks—experimental evidence for the physical mechanism of the formation of a jam. New journal of physics, 10(3):033001, 2008.

[35] Xiaotian Sun, Laura Muñoz, and Roberto Horowitz. Highway traffic state estimation using improved mixture kalman filters for effective ramp metering control. In 42nd IEEE International Conference on Decision and Control (IEEE Cat. No. 03CH37475), volume 6, pages 6333–6338. IEEE, 2003.

[36] Shin-ichi Tadaki, Macoto Kikuchi, Minoru Fukui, Akihiro Nakayama, Katsuhiro Nishinari, Akihiro Shibata, Yuki Sugiyama, Taturu Yosida, and Satoshi Yukawa. Phase transition in traffic jam experiment on a circuit. New Journal of Physics, 15(10):103034, 2013.

[37] Alireza Talebpour and Hani S Mahmassani. Influence of connected and autonomous vehicles on traffic flow stability and throughput. Transportation Research Part C: Emerging Technologies, 71:143–163, 2016.

[38] Meng Wang, Winnie Daamen, Serge P Hoogendoorn, and Bart van Arem. Cooperative car-following control: Distributed algorithm and impact on moving jam features. IEEE Transactions on Intelligent Transportation Systems, 17(5):1459–1471, 2015.

[39] Fangyu Wu, Raphael Stern, Miles Churchill, Maria Laura Delle Monache, Ke Han, Benedetto Piccoli, and Daniel B Work. Measuring trajectories and fuel consumption in oscillatory traffic: Experimental results. Transportation Research Board Annual Meeting, 2017.

[40] Yang Zheng, Jiawei Wang, and Keqiang Li. Smoothing traffic flow via control of autonomous vehicles. IEEE Internet of Things Journal, 7(5):3882–3896, 2020.